Investigations into the behaviours of Coriolis flowmeters under air-water two-phase flow conditions on an optimized experimental platform

Jinyu Liu[a], Tao Wang[b], Yong Yan[a*], Xue Wang[c], Lijuan Wang[a]

[a] School of Engineering and Digital Arts
University of Kent
Canterbury, Kent CT2 7NT, U.K.

[b] KROHNE Ltd.
Wellingborough NN8 6AE, U.K.

[c] School of Mathematics, Statistics and Actuarial Science
University of Kent
Canterbury, Kent CT2 7NT, U.K.

Abstract—Gas-liquid two-phase flow is commonly encountered in many industrial processes due to production requirement or inevitable gas entrainment from various sources. Accurate liquid phase measurement under two-phase conditions is challenging but important as it is the key factor to reduce cost, improve safety or meet legal requirements. Coriolis flowmeters, owing to their high accuracy in metering single-phase flow, direct mass flow measurement and multivariable sensing nature, are widely used in industry. Recently developed Coriolis flowmeters can work under multiphase conditions, making it possible to achieve accurate multiphase flow measurement through model based error compensation or training based soft computing correction. This paper assesses the behaviours of Coriolis flowmeters under various two-phase conditions for modelling and soft computing algorithm improvement, including previously investigated factors (flowrate, gas volume fraction, flow tube geometry, flow converter, and process pressure) and new factors (flow regimes in terms of bubble size and distribution). Experimental work was conducted on 25 mm and 50 mm bore air-water two-phase flow rigs for liquid mass flowrates between 2500 kg/h and 35000 kg/h with gas volume fraction of 0-60%. With the influence of each factor identified through univariate analysis, comparisons between existing modelling theories and experimental error curves are established. In the meantime, the rig design and control are optimized to provide efficient and automated data acquisition in order to supply ample and high-quality data for the training of soft computing models as well as enhancing the understanding in theoretical modelling.

Keywords—air-water two-phase flow; Coriolis mass flowmeter; modelling; soft computing; flow rig

I. INTRODUCTION

Gas-liquid two-phase flow often occurs in many industrial processes such as oil and gas exploration, chemical engineering and food processing, where accurate flow measurement is required for various reasons, including meeting legal requirements. For example, in the oil and gas industry, an additional 0.1% measurement error would lead to $78.8 billion financial exposure per year for a single pump station [1]. However, despite significant effort in research in multiphase flow metering, the measurement accuracy of existing multiphase flowmeters is still far from the required accuracy for the purpose of accounting. An ideal candidate to address the multiphase flow measurement problem is the Coriolis flowmeter. As the most accurate single-phase mass flowmeter, Coriolis flowmeters not only output directly mass flowrate which can be immune to changes in temperature and pressure but also provide independent density measurement of the fluid. Meanwhile, signals from other parts of a Coriolis flowmeter, including its exciter and sensors, also provide useful diagnosis information such as damping, asymmetry, imbalance, etc.

Investigations into the performance of Coriolis flowmeters under two-phase conditions exist for decades [2]. Under real industrial process conditions, single-phase liquid to be measured is often subjected to inevitable gas entrainment from various sources. Consequently, the measurement accuracy of a Coriolis flowmeter deteriorates dramatically from ±0.1% to unacceptable level with minimum gas entrainment (1~2% gas by volume) and the flowmeters even stopped working completely with excessive gas entrainment [3]. Recently, with the advances in digital converters [4], new generation Coriolis flowmeters no longer cease working under multiphase flow conditions but large measurement errors are expected, motivating research in accuracy improvements in two categories: development of a sensor system/theory based model or an empirical/data-driven model to compensate existing errors. Although a universally adapted two-phase flow correction model would be ideal and is the ultimate goal, existing theoretical error models [5]-[11] have achieved limited success due to complex phase interactions commonly seen in multiphase flow. Rigorous assumptions have to be made such as evenly distributed bubbles far away from tube wall and each other in order to derive an expected flowmeter output error, which usually do not hold even in laboratory conditions. Most recently, a Coriolis flowmeter centred measurement system incorporating soft computing algorithms has achieved real-time ±1% liquid measurement

* Corresponding author: Email: Y.Yan@kent.ac.uk ;Tel: +44 (0) 1227 823015

error and ±10% gas volume fraction (GVF) estimation in air-water two-phase flow on a 25 mm bore rig [12] or ±2.5% liquid phase flowrate, ±5% gas phase flowrate measurement error in oil-gas-water multiphase flow [13]. Promising as such, soft computing methods are based on input-output mapping, depending significantly on similarities between training and application scenario. Factors such as flowrate, apparent density, differential pressure across the Coriolis flowmeter are included in soft computing training [12], [14]-[17], but more factors need to be identified and their effects taken into account in developing soft computing models. Experimental data from existing two-phase flow rigs [12], [18], [19] have revealed the error curve dependency on flowrate, GVF, meter installation orientation, flow tube geometry, flow converter and fluid viscosity. Meanwhile, other factors such as inlet and outlet pressures and repetitive tests under same conditions do not alter error curves significantly [18], [19].

In this paper, we apply for the first time a univariate approach to experimentally investigating the key factors that affect the mass flow error curves of Coriolis flowmeters. This involves new parameters or conditions that have not been considered in all earlier studies such as flow regimes in terms of bubble size and distribution. In addition, previously investigated key factors, including liquid flowrate, GVF, flow tube geometry, flow converter and process pressure, are also assessed for purpose of comparisons. As a result, this study would provide new experimental results and ample training data under various test conditions for a soft-computing model, leading to future improvements in theoretical modelling.

II. Methodology

The factors that affect the mass flow error curves are selected and inspected one at a time to experimentally observe their influences on the mass flowrate error curves. These factors include variations in liquid flowrate, amount of gas entrained, pressure, different flow regimes and flow tube geometry, some of which were mentioned in existing modelling theories [5]-[11]. Consequently, the new experimental results are used for interpretation of theoretical models and training of soft computing models.

Two established error theories include decoupling and compressibility errors [5]-[11], which are briefly reviewed here. Firstly, the derived decoupling error due to gas-liquid phase relative motion radially is

$$E_d = \frac{1-F}{1-\alpha}\,\alpha \tag{1}$$

where α is cross-sectional void fraction assuming GVF equals void fraction under homogeneous flow. This is true under most of the test conditions in this paper, if no slip between gas and liquid phase is assumed. It also defines a gas-liquid decoupling ratio F (gas bubble vibration amplitude over liquid vibration amplitude) between 1 and 3 to describe the phase radial relative motion, which is further modelled to correlate to the inverse Stoke number, or the normalised viscous penetration depth

$$\delta = \frac{1}{r}\sqrt{\frac{2\nu}{\omega}} \tag{2}$$

where ν, ω and r are kinematic fluid viscosity, tube vibration frequency, and bubble radius assuming spherical bubbles, respectively. Secondly, the compressibility error is

$$E_C = \frac{1}{2}\left(\frac{\omega}{c}b\right)^2 \tag{3}$$

where c and b are mixture speed of sound and tube radius, respectively. E_C describes a positive error caused by compressibility increase in gas-liquid mixture. Even though the assumptions of these theoretical equations are often limited, at least they identified the relevant parameters and provided a way to correlate between parameters and error curve changes.

The liquid flowrate variation range is chosen according to the single-phase nominal range and turn down ratio of a Coriolis flowmeter. Pressure and GVF variation range are chosen to reflect real industrial situations as well as considering the limitation of the test rig. This will ensure the outcome of this research is valid for actual applications. Additionally, variations in flow regimes, liquid viscosity (excluded due to rig limitation), vibration frequency and tube diameter of the Coriolis flowmeter should also be investigated as they are relevant to existing error prediction theories. TABLE I. summarizes the conditions under which the experimental tests were undertaken.

TABLE I. Experimental conditions

Component	**Specification**	
Water flowrate	50 mm rig	5000-35000 kg/h
	25 mm rig	2500-15000 kg/h
Air flowrate	5-160 nl/min	
GVF	0-60 %	
Pressure	20 kPa, 300 kPa	
Flow conditioners	Swirl, Grid, Hybrid; Installed near (0 mm) and far (1000 mm) from the Coriolis flowmeter under test	
Flow tube geometry and flow converter	Meter A~C from different manufacturers	
Air injection point	Inject air from top and bottom, near and far from the Coriolis flowmeter under test (500 mm difference)	
Upstream straight-section length	250 mm, 1250 mm	

Experiments are designed to change flowrate, GVF, pressure (by controlling pump speed and valve opening), flow regimes (by changing flow conditioner, upstream straight-section length, air injection location and pressure), ω and b together with flow tube geometry and flow converter (by changing Coriolis flowmeters from different manufacturers). During the experiments, raw output data from all flowmeters and rig configurations were recorded for the training of soft computing models as well as replicating test conditions for real-time performance evaluation of soft computing models. These raw data are then averaged over one minute and plotted for error curve analysis.

III. Experimental Results and Discussion

A. Test Facility and Test Conditions

Fig. 1 shows the schematic of the air-water two-phase flow test rig whilst Fig. 2 is a photo of the 50 mm bore test section. Two experimental rigs were used with different bore test sections (25 mm and 50 mm), offering single-phase uncertainties of 0.035%. Each rig consists of a Coriolis flowmeter and a thermal mass flowmeter to provide single-phase water and air references before mixing. A simple tee was used for injecting air into liquid at different locations and directions. The fluid with known liquid mass flowrate and GVF was then fed to the Coriolis flowmeter under test to evaluate measurement error under two-phase conditions. To best estimate the GVF, pressure downstream of the meter under test and temperature of meter under test are used to infer air volume inside meter tubes thus GVF assuming no slip between air and water phase. In addition, a differential-pressure measurement across the Coriolis flowmeter was taken to capture more information regarding flowrate, GVF and pressure fluctuation. Additional temperature and pressure transducers were also installed to record the process conditions. Outside the test section, an upstream centrifugal pump and a downstream regulation valve were used to control water flowrate and process pressure.

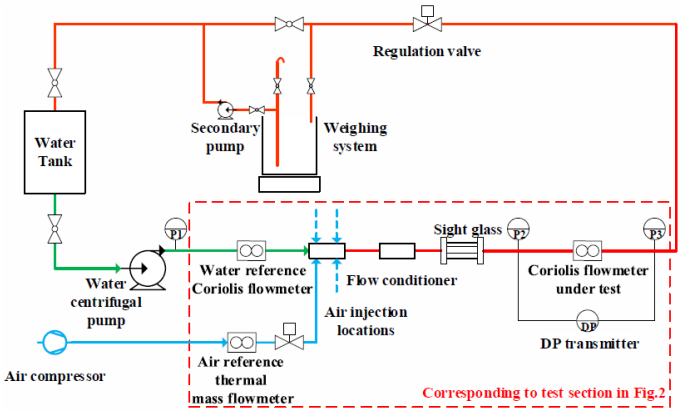

Fig. 1. Schematic of the air-water two-phase flow rig.

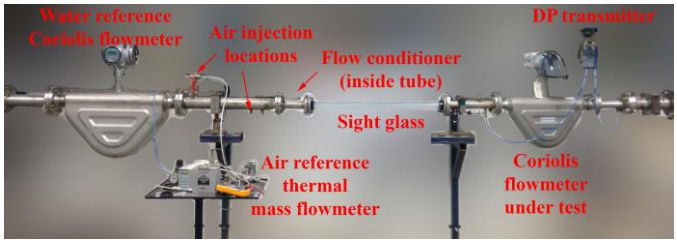

Fig. 2. Photo of the experimental test section in Fig. 1.

In order to produce high quality data for error curve interpretation and soft computing model training, data are featured with broad range, univariate in nature, high accuracy, good repeatability and large in quantity. Through automated control of all liquid and air reference flowrates and back pressure by using three independent proportional–integral (PI) controllers, processes that commonly seen in industry covering bubbly, slug and dispersed flow regimes were reproduced on the rigs. Several rig repeatability tests shown in Fig. 3 indicate that the maximum deviation of water reference flowrate at different GVF is 1.85%, which could have been 20.16% without the PI controllers to compensate the increased resistance due to higher GVF. The maximum deviation of back pressure is 1.85%, improved from 130% without automation by PI controllers (compared with averaged back pressure among each test). Besides, by characterizing pump speed, valve opening with corresponding flowrate, back pressure, guided initial pump and valve values were given before handing over to automatic PI controllers, which reduced the overall test durations.

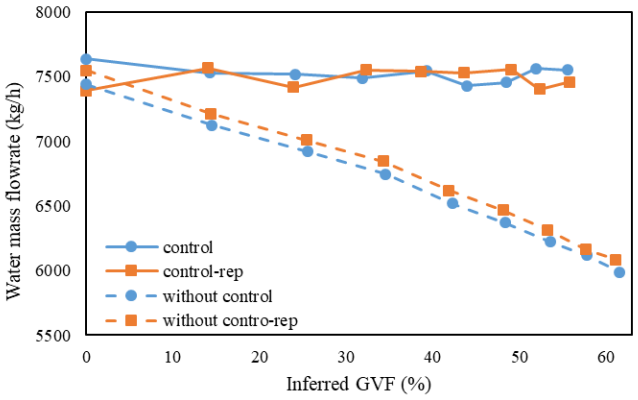

(a)

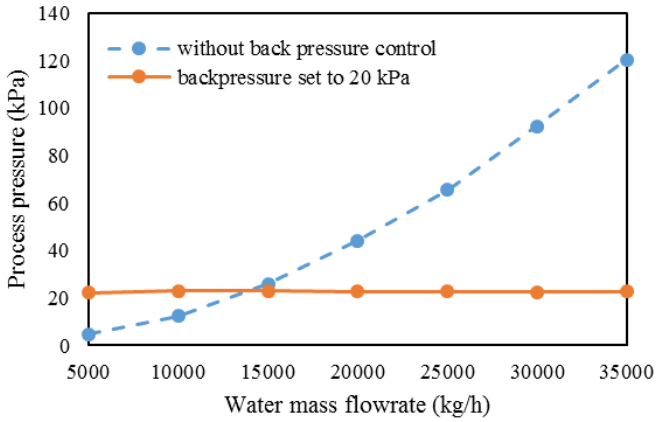

(b)

Fig. 3. Stability and repeatability evaluation of (a) reference flowrate of water and (b) back pressure with and without control.

B. Benchmark Tests

Benchmark tests were conducted to rule out factors that do not contribute to error curve differences.

Modern flow converters (or transmitters) from different Coriolis flowmeter manufacturers have a minimized effect on error curve difference as shown in Fig. 4. When the converter on Meter B is replaced by converter from Meter A, the outputs based on the same signals are similar. Some large differences are expected due to greater fluctuations under higher GVFs. Similar conclusion applies to Meter A and Meter C comparison.

Repeat the test under the same condition will reproduce similar flow error curves. One set of repeatability tests using the density reading from the meter under test to estimate apparent GVF is shown in Fig. 5. Results in Fig. 5 show that the maximum difference is 3% at high apparent GVF (43.3%) while

the averaged difference is 0.1%. Except for the large error curve difference at high GVF due to low signal to noise ratio and fluctuation, the repeatability result endorses the credibility of the test data.

Process pressure has noticeable effect on air volume but it has been taken into account in GVF calculation. Results show that variation of pressure from 20 kPa to 300 kPa lead to a maximum error curve difference of 6%.

Air injection direction and location would affect the flow regime but this effect is weakened by the straight test section and mixers upstream of Coriolis flowmeters. As a result, changing in air injection direction and location is observed to cause a maximum error curve difference of 5%.

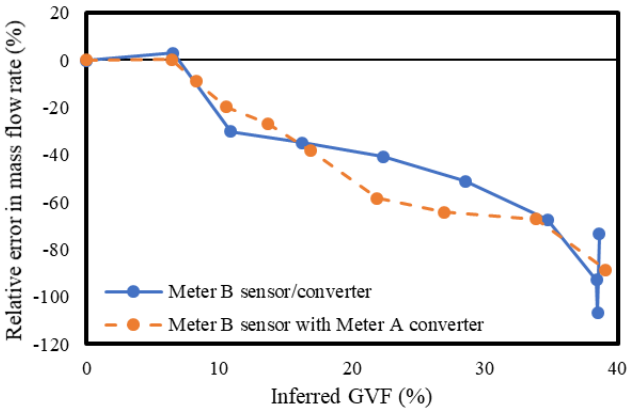

Fig. 4. Results from different converters on the same flow sensor.

High viscosity of the fluid being measured would reduce decoupling error thus lead to more positive error, which shows a maximum error curve difference of 40% through comparison between Fig. 1 and Fig.8 in [19].

The meter orientation will also affect error curve as a result of changes in bubble size and its distribution and flow regime. Henry et al. [19] showed a maximum error curve difference of 20% under different flowmeter orientations while a later generation of Coriolis flowmeter showed a maximum error curve difference of 20% [12] and 5.5% [18] under different flowmeter orientations.

From the next section, factors affecting the performance of the Coriolis flowmeter will be investigated by altering one factor at a time. Previously explored factors [12], [18], [19] together with factors considered in this paper are listed in TABLE II.

TABLE II. EXPERIMENTAL CONDITIONS AND THEIR EFFECTS

Behaviour affected?	**Variations in test conditions**	
	In the literature [12], [18], [19]	***In this paper***
Yes	flowrate [12], [18], [19]; GVF [12], [18], [19]; meter size [19]; flow tube geometry [19];	
	viscosity [19]; flow converter [19]; orientation [12], [18], [19]	flow regimes in terms of bubble size and distribution
No	process pressure [19]; repeated tests [18]	
	-	flow converter; air injection direction and location

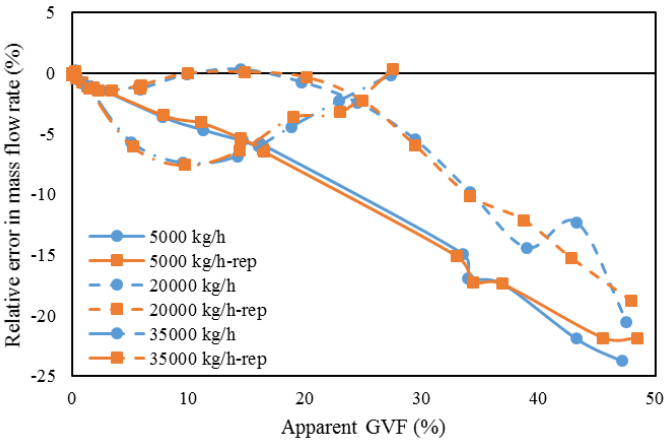

Fig. 5. Error curve repeatability evaluation.

C. *Effect of GVF and Flowrate*

Fig. 6 shows that the typical mass flowrate error curves depend on GVF and flowrate. It becomes clear that either the decoupling error in (1) or the compressibility error in (3) alone cannot predict these error curves. The combination of both types of errors could be used to explain the error curves instead. For most of the flowrates except for lowest flowrates, decoupling errors dominate the error curves, leading to around 3α negative errors for low GVFs. Then with increased GVFs, compressibility errors are increased, offsetting decoupling errors and even dominate at certain stage. With further GVFs increase, positive compressibility errors according to equation (3) increase much slower than decoupling errors causing overall negative errors at high GVFs. However, for low flowrates, the positive errors emerge much earlier at low GVFs. One possible explanation would be that the slug flow regime at low flowrate suppresses decoupling errors but enhances compressibility errors. In addition to these two types of errors, another error source is the asymmetric damping, but there is not a theoretical model to describe such a mechanism. It is worth noting that low Reynolds numbers may affect Coriolis flow measurement in particular for large size meters [2]. In our experimental setup the Reynolds number ranges from 26,000 to 280,000 so that the effect of the Reynolds number is insignificant in this study.

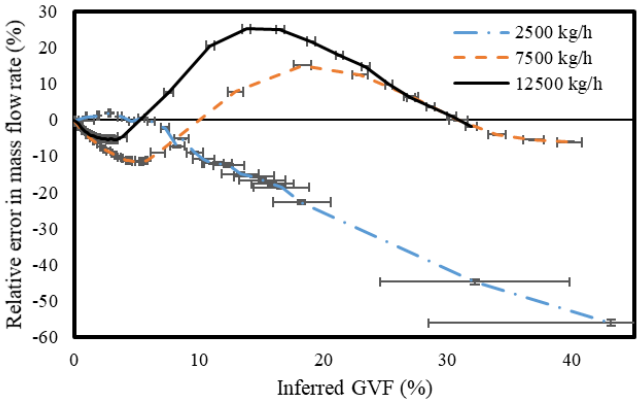

Fig. 6. Effect of different GVF and flowrate.

D. *Effect of Flow Regime (conditioner)*

An alternative way of changing flow regimes under the same process conditions would be using different flow conditioners of complex shapes made by 3D printing. A swirl mixer consisting of four 180° helical sections with the same twist direction shown in Fig. 7 (a) was used. Due to centrifugal forces, the gas phase is concentrated in the centre of the pipe. A grid mixer consisting of corrugated plates shown in Fig. 7 (b) was also used. It breaks bubbles into smaller sizes and makes bubbles evenly distributed in the pipe. A hybrid mixer which combines a half-length swirl mixer and another half-length grid mixer was then used in the tests. These mixers along with no mixer configurations were tested with different upstream straight-section lengths. Two examples of the resulting bubble size and distribution are shown in Fig. 8.

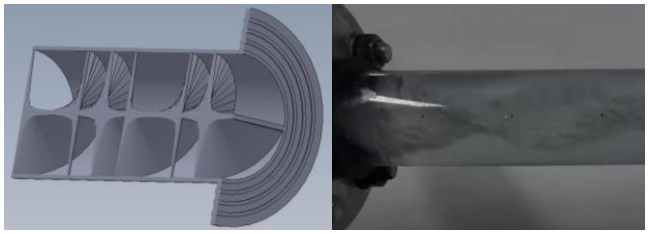

(a)

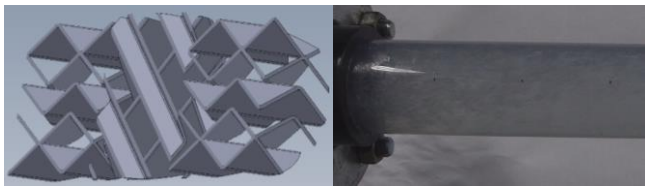

(b)

Fig. 7. Sectional views of (a) swirl and (b) grid flow conditioners with flow regimes under 5000 kg/h flowrate and 900 kg/m^3 apparent density.

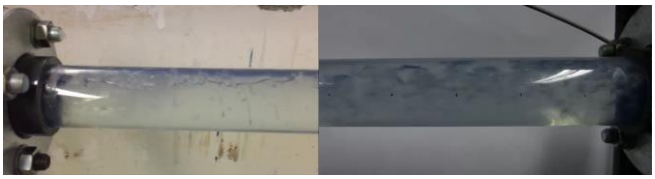

Fig. 8. Flow regimes without flow conditioner (left) and with swirl mixer after the one meter long upstream straight-section tube (right).

From the sight glass, we observed that the large bubbles are distributed in the middle of the tube for a long time after the swirl mixer while small bubbles are evenly distributed and rise up much faster after the grid mixer. For the no mixer condition or after the one meter long straight-section tube shown in Fig. 8, bubbles are noticeably different in size and appear on the top of the pipe compared to the flow regimes immediately downstream of the mixers. Fig. 9 shows the resulting mass flowrate error curves affected by flow conditioners and their installation locations for a typical liquid reference flowrate. This maximum error curve difference of 25% is largely due to bubble size and depends on GVF. The upstream grid mixer installed near the meter allow less time for bubbles to merge back to big ones. As a result, a grid mixer installed near the Coriolis flowmeter would result in smaller bubbles inside the flowmeter, thus less negative decoupling errors according to equations (1) and (2). With a longer straight-section tube, no mixer or swirl mixer configuration, larger bubbles inside the flowmeter result in more negative decoupling errors. It is worth mentioning that the bubble size is still affected by flowrate and the error curve is different under different water flowrates. Although it is an inferred conclusion from existing theories without measuring bubble sizes, the results show that the variation of upstream flow regimes could lead to distinguished error curves, which is difficult to be accommodated by a soft computing model if the training was taken place under a different upstream flow regime. Further attempts could include bubble size measurement using a high speed camera or to explore if other diagnostic signals inside Coriolis flowmeters could distinguish different upstream flow regimes. Moreover, the deviation between theory and experimental results could also be the consequence of other factors not taken into account during modelling such as fluid asymmetrically distributed along the tube or unevenly distributed between tubes or external disturbances.

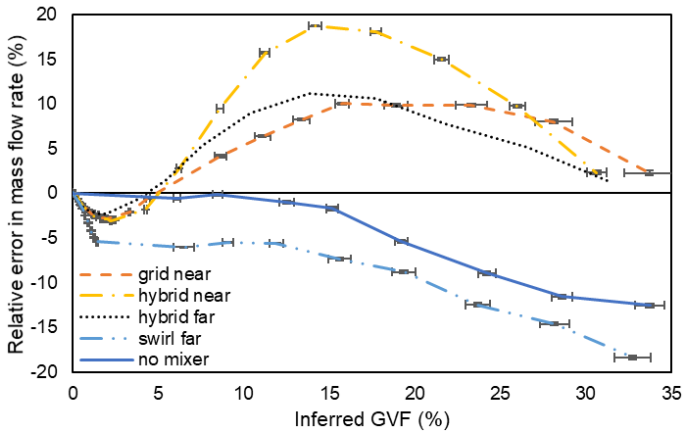

Fig. 9. Responses of Coriolis flowmeters to different flow conditioners at 15000 kg/h water flowrate.

E. *Effects of Flow Sensor Design*

The Coriolis flow sensors from different manufacturers are evaluated to cause a maximum error curve difference of 60% in mass flowrate, where Meter A uses 'V'-shaped (shallow bend angle) twin bent-tubes with an internal tube diameter of 22 mm whilst Meter B is based on 'U'-shaped (deep bend angle) twin bent-tubes with an inner diameter of 20 mm. Additionally, the drive frequency of Meter A with water is 240 Hz, while the drive frequency of Meter B is 260 Hz. Meter B was installed upstream of Meter A for the first experiment and meter positions were swapped for a second identical experiment. Fig. 10 shows the different error curves of Coriolis flowmeters from different manufacturers under the same experimental conditions. As the effects of flow converters are ruled out in the benchmark test section, flow regimes inside the flow tubes affected by its geometry are mainly responsible for the difference in error curves. In addition, since the upstream twin-tube Coriolis flowmeter can be regarded as a mixer similar to a grid mixer for the downstream Coriolis flowmeter, the increase in positive error when the Coriolis flowmeter is at downstream also supports hypothesis in Section III. D.

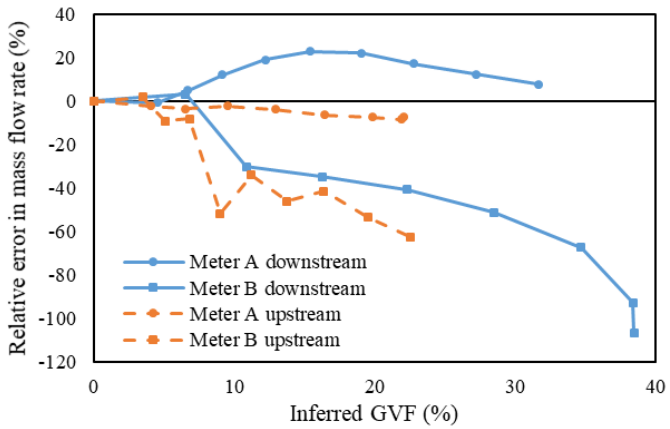

Fig. 10. Results from different manufacturers.

IV. Conclusions

In this paper, factors that affect the behaviours of Coriolis flowmeters, including flowrate, GVF, flow regimes and Coriolis flow tube geometry, have been investigated. Although the maximum error as large as 60% and 50% over the range of GVF and flowrate can be compensated by soft computing algorithms [12], the method requires the error curve to be reproducible under training and testing conditions. Experimental results in this paper have shown the maximum error curve difference can be 60% and 25% under different flow tube geometries and flow conditioners, respectively, which could lead to significant output errors if compensated according to the error curve without considering these two factors. Therefore, the investigations conducted in this paper provide more training scenarios thus suitable error curves under each test condition for the improvement of soft computing models. In addition, attempts have been made to correlate the variations of error curves with existing theories. Furthermore, the importance of automating the experimental procedure to efficiently obtain a large volume of data was highlighted. Future work will include the improvement in the generalization capability of soft computing models on new test data and theoretical models.

References

[1] E. Dupuis. “Oil and gas custody transfer when money changes hands, flow measurement accuracy matters.” Internet: http://www2.emersonprocess.com/siteadmincenter/PM%20Articles/Oil-and-Gas-Custody-Transfer_petroleum_africa_may_2014.pdf, [Accessed: 30- Oct- 2017].

[2] T. Wang, R. Baker, “Coriolis flowmeters: a review of developments over the past 20 years, and an assessment of the state of the art and likely future directions,” Flow Meas. Instrum., vol. 40, pp. 99-123, 2014.

[3] J. R. Reizner, “Exposing Coriolis mass flowmeters' “dirty little secret”,” Chem. Eng. Prog., vol. 100, no.3, pp. 24-30, 2004.

[4] M. P. Henry, D. W. Clarke, N. Archer, J. Bowles, M. J. Leahy, R. P. Liu, J. Vignos, F. B. Zhou, “A self-validating digital Coriolis mass-flow meter: an overview,” Control Eng. Pract., vol. 8, no.5, pp. 487-506, 2000.

[5] J. Hemp and H. Yeung, “Coriolis meters in two phase conditions,” Comput. Control Eng. J., vol. 14, no.4, pp. 36-36, 2003.

[6] J. Hemp, J. Kutin, “Theory of errors in Coriolis flowmeter readings due to compressibility of the fluid being metered,” Flow Meas. Instrum., vol. 17, no.6, pp. 359-369, 2006.

[7] N. T. Basse, “A review of the theory of Coriolis flowmeter measurement errors due to entrained particles,” Flow Meas. Instrum., vol. 37, pp. 107-118, 2014.

[8] N. T. Basse, “Coriolis flowmeter damping for two-phase flow due to decoupling,” Flow Meas. Instrum., vol. 52, pp. 40-52, 2016.

[9] D. L. Gysling, “An aeroelastic model of Coriolis mass and density meters operating on aerated mixtures,” Flow Meas. Instrum., vol. 18, no.2, pp. 69-77, 2007.

[10] A. Rieder, H. Zhu and W. Drahm, “Coriolis mass flowmeters: on measurement errors in two-phase conditions," in Proc. of the 13th Int. Flow Measurement Conf., Peebles, Scotland, 6-9 June 2005.

[11] J. A. Weinstein, D. R. Kassoy and M. J. Bell, “Experimental study of oscillatory motion of particles and bubbles with applications to Coriolis flow meters,” Phys. Fluids, vol. 20, no. 10, 2008

[12] L. Wang, J. Liu, Y. Yan, X. Wang and T. Wang, “Gas-liquid two-phase flow measurement using Coriolis flowmeters incorporating artificial neural network, support vector machine, and genetic programming algorithms,” IEEE Trans. Instrum. Meas., vol. 66, no.5, pp. 852-868, 2017.

[13] M. Henry, M. Tombs and F. Zhou, “Field experience of well testing using multiphase Coriolis metering,” Flow Meas. Instrum., vol. 52, pp. 121-136, 2016.

[14] R. Liu, M. Fuent, M. Henry and M. Duta, “A neural network to correct mass flow errors caused by two-phase flow in a digital coriolis mass flowmeter,” Flow Meas. Instrum., vol. 12, no.1, pp. 53-63, 2001.

[15] Q. Hou, K. Xu, M. Fang, Y. Shi, B. Tao and R. Jiang, “Gas-liquid two-phase flow correction method for digital CMF,” IEEE Trans. Instrum. Meas., vol. 63, no. 10, pp. 2396-2404, 2014.

[16] L. Ma, “Mass flow measurement of oil-water two-phase flow based on coriolis flow meter and SVM,” Journal of Chemical Engineering of Chinese Universities, vol. 21, no.2, pp. 201-205, 2007.

[17] L. Xing, Y. Geng, C. Hua, H. Zhu and A. Rieder, “A combination method for metering gas–liquid two-phase flows of low liquid loading applying ultrasonic and Coriolis flowmeters,” Flow Meas. Instrum., vol. 37, pp. 135-143, 2014.

[18] J. W. Kunze, R. Storm and T. Wang, “Coriolis mass flow measurement with entrained gas, ”, in Proc. of Sensors and Measuring Systems, pp.1-6, Nuremberg, Germany, 3-4 June 2014.

[19] M. Henry, M. Tombs, M. Duta, F. Zhou, R. Mercado, F. Kenyery, J. Shen, M. Morles, C. Garcia, R. Langansan, “Two-phase flow metering of heavy oil using a Coriolis mass flow meter: A case study,” Flow Meas. Instrum.,vol. 17, no. 6, pp. 399-413, 2006.